Long-Term Measurement of PMD and Polarization Drift in Installed Fibers

Magnus Karlsson, Jonas Brentel, and Peter A. Andrekson, *Member, IEEE*

***Abstract*—We report the most detailed long-term measurement of polarization mode dispersion (PMD) made to date. We measured two separate fibers under the same time period, which makes it possible to compare the drift properties of two similar fibers in the same environment. The measured Jones matrices suffers from both random and systematic errors, a generic problem which we discuss in detail and solve. The results confirmed the well-known statistical properties of the PMD-vector. Furthermore, the drift averaged over wavelength is very well (96%) correlated between the two fibers. We finally quantified the temporal drift by computing the autocorrelation function of the PMD-vector analytically, both with respect to wavelength and to drift time. The analytical theory shows good agreement with the measurements.**

***Index Terms*—Fiber characterization, polarization drift, polarization-mode dispersion (PMD).**

I. Introduction

POLARIZATION-MODE dispersion (PMD) is commonly regarded as one of the most serious obstacles facing future high-speed fiber transmission. It is particularly difficult to compensate for since it varies with wavelength and slowly drifts with time in a random fashion. To establish the impairments from PMD on transmission systems, one then must resort to statistics, and it is obviously important to have a clear picture of the statistical properties of PMD.

It is the drift of the polarization properties with time that is the most troublesome aspect of PMD from a system point of view. A deterministic birefringence would be fairly straightforward to compensate for (at least over moderate bandwidths), but when the birefringence drifts the compensation scheme must adjust and dynamically follow this drift. This tends to make realizations of effective PMD compensators complex and expensive.

Another problem with PMD is that cabled fiber in the ground and spooled fiber in the lab differ in several important aspects, such as the mode coupling lengths and the drift properties. It is therefore of additional importance to characterize installed fibers rather than lab fibers. The drift of the PMD in installed fiber have been investigated by several groups, but several questions remain unsolved. For instance, what is the origin of the drift? How fast is the drift, and what additional fiber properties determines the drift? Does the PMD drift on the same time scale as the absolute polarization state? The purpose of this paper is to, if not straighten out all question marks, at least shed some light over these rather difficult issues.

Manuscript received November 4, 1999; revised March 28, 2000. This work was supported by the Swedish Research Council for Engineering Sciences (TFR), the Swedish Board for Industrial and Technical Development (NUTEK), and the ACTS project Multi-gigabit Interconnection using Dispersion compensation and Advanced Soliton techniques (MIDAS).

The authors are with the Department of Microelectronics, Photonics Laboratory, Chalmers University of Technology, Göteborg S-412 96, Sweden.

Publisher Item Identifier S 0733-8724(00)05760-1.

A. Properties of the PMD-Vector

The effects of PMD is treated by means of the *PMD-vector*, $\boldsymbol{\Omega}(z, t, \omega)$, which is a 3-component polarization vector in Stokes space. It varies in a random fashion with fiber length z, the optical frequency ω and time t. In a practical transmission situation, the fiber length z is constant, and only the drift and frequency variation of $\boldsymbol{\Omega}$ are of interest. Given a constant input polarization to the fiber, PMD will manifest as a change in output polarization Stokes vector $\boldsymbol{s}$ with frequency according to $\boldsymbol{s}'(\omega) = \boldsymbol{\Omega} \times \boldsymbol{s}(\omega)$. This equation might in fact be taken as the definition of the PMD vector, but the reader should note that the definition is restricted to the case of fibers with negligible polarization-dependent loss (which is no serious limitation in most transmission systems). Apart from this, the above definition has a lot of advantages: First, it is the underlying model for most statistical treatments of PMD [1]–[3] and thus it forms the basis for most of the known statistical properties of the PMD-vector. Second, it is the definition used in the Jones-matrix method [4], which is more or less regarded as the reference measurement method for PMD. Third, this definition provides a very elegant concatenation rule for the PMD-vector of a sequence of birefringent elements [5], [6]. Fourth, and finally, this definition provides a comfortable way of calculating the PMD-induced broadening and group delay of short polarized pulses via integrals of the PMD-vector over the pulse spectrum [7]. For example, the group delay of a pulse with polarization vector $\boldsymbol{j}$ is $\langle \boldsymbol{\Omega} \rangle \cdot \boldsymbol{j}/2$, where $\langle\, \rangle$ denotes integration over the normalized pulse spectrum. The drawback of this definition of the PMD-vector is that the incorporation of polarization-dependent losses (PDL) is far from straightforward, and a simple and elegant way of accounting for both PMD and PDL is yet to be found. In this paper we assume PDL to be negligible, an assumption that was also verified in the measurements.

Obviously, the polarization states parallel and antiparallel with the PMD-vector will (to first order in ω) not change with wavelength, and those states are called the *principal states of polarization* (PSP's). From the defining equation we can also conclude that the length of the PMD vector [called the differential group delay (DGD), $\Delta\tau$] determines the rate of polarization change with frequency. In the time domain, $\Delta\tau$ will be the group delay between light polarized along the two PSP's.

0733–8724/00$10.00 © 2000 IEEE

B. Polarization Fluctuations in Fibers

Long-term measurements of the polarization properties of installed fibers have been done on many instances with more or less inconsistent results. The first such measurements were reported in the eighties [8]–[12], and focused on the drift of the absolute polarization state after different lengths of installed (mostly submarine) single-mode fibers. It was found that the drift for installed fibers was rather slow; on the order of hours to days [8]–[12]. It was also argued theoretically [11] and experimentally [10] that the variance of the fluctuations grew linearly with the fiber length. More rapid drifts (on second timescales) were observed on cables subjected to rapid environmental changes, e.g., during installation of submarine cables [13], [14], for applied vibrations [15] and other perturbations such as stress, temperature changes, etc. [16].

It is not obvious that this kind of fluctuations of the absolute polarization state also will affect the PMD, since it is well-known that the DGD is unaffected by, e.g., the presence of a polarization controller at one end of a fiber under PMD measurement. However, the PMD-vector is not unaffected by such a polarization controller, and we will therefore discuss this in some more depth.

We first consider a single pointwise fluctuation (it can be thought of as a fluctuating polarization controller) at a distance h from the source, along a fiber of length L. The total PMD-vector of the fiber can be written as a vector sum of the PMD vector of the first part (call it $\mathbf{\Omega}_1$) and the PMD-vector of the second part (call it $\mathbf{\Omega}_2$). For an exact concatenation rule we refer to the appendix or Ref [6]. Here it suffices to state that the total PMD vector will be $\mathbf{\Omega}_{\rm tot} = \mathbf{\Omega}_1 + M\mathbf{\Omega}_2$, where M is some arbitrary rotation (or Mueller) matrix. From a simple geometrical picture it is evident that the maximum and minimum values of the total DGD $|\mathbf{\Omega}_{\rm tot}|$ will be the sum and difference of the two partial DGD:s, i.e., $||\mathbf{\Omega}_1| \pm |\mathbf{\Omega}_2|| = |\Delta\tau_1 \pm \Delta\tau_2|$, and the average will be the quadratic sum, i.e., $E[|\mathbf{\Omega}_{\rm tot}|] = \sqrt{\Delta\tau_1^2 + \Delta\tau_2^2}$. It is straightforward to show that the maximum fluctuation in the length of $\mathbf{\Omega}_{\rm tot}$ (the total DGD) will occur for $\Delta\tau_1 = \Delta\tau_2$, i.e. when $h = L/2$. The direction of the PMD vector will in this case only fluctuate $180°$, i.e., within a half plane. In the other limit, when the point of fluctuation is at either end point ($h = 0$ or $h = L$) the length of the total PMD is unchanged, but the direction might vary over the entire $360°$ of the Poincaré sphere. Hence, depending on the position of the fluctuation, the DGD and the PSP's are affected in various amounts. Now, in a realistic fiber the fluctuation points are likely to be evenly distributed over the entire fiber length, so fluctuations are likely to arise in both the length and the direction of the PMD-vector at the same time. Moreover, any polarization fluctuation (independently of h) will affect also the *absolute* output polarization state and cause it to vary randomly over the Poincaré sphere. The time scale of such fluctuations will therefore be slightly faster but on a similar time scale as the PMD-vector fluctuations.

C. Motivation and Outline of This Work

This paper aims to investigate the fluctuations of the PMD-vector in installed fibers in more detail. When investigating the literature on this subject [17]–[26] one finds an interesting variation concerning the speed of the PMD drift in installed fibers. Some measurements report rapid time variations; over minutes and shorter [17]–[23], and in a few cases the DGD have found to be constant over days and more [24], [25]. The consensus on the subject is that rapid variations occur for transmission lines (or parts thereof [18]) which have been exposed to mechanical perturbations (e.g. aerial cables [22], or significant day-night temperature changes [17], [18]. The stable cables were buried under ground [25], or sub-marine [24]. It is also commonly believed that the rate of temporal change increases with the cable length and the PMD, although there are not yet any theoretical foundations for that. Finally, the average of the DGD over a sufficiently wide wavelength interval has been shown to be more or less unaffected by temporal drifts [26]. Here "sufficiently wide" means that it should occupy several autocorrelation lengths of the PMD vector, which was recently calculated to be of the order of the inverse average DGD [6].

In order to investigate the drift properties further, we have conducted a long-term PMD measurement on two fibers in the same cable simultaneously. This measurement, which we believe is the most detailed to date, provides us with sufficiently many measured points to reliably check the statistical properties of the PMD vector and its drift. We also aim at a more detailed theoretical understanding of the drift, in terms of a correlation time of the PMD-vector.

The second section of this paper contains a detailed description of the measurement and the analysis we performed on the measured data. The latter is nontrivial, because the measured Jones matrices were found to contain both systematic and random errors, the handling of which we believe is of general interest. The third section discusses the result of the measurement, verifies (for the first time) the isotropicity of the PMD vector and demonstrates the good correlation between the two fibers with respect to drift. The fourth and final section discusses the drift in terms of auto correlation functions (ACF:s), and compares the measured ACF with the theoretically predicted one. A comprehensive derivation of the ACF with discussions on basic assumptions and validity of the theory is deferred to the Appendix. Here we also can find a confirmation of the "common belief" that the fluctuations due to the drift increases with the PMD and the fiber length, and the theory will also connect the fluctuation times of the absolute polarization state with that of the PMD-vector.

II. Measurement and Data Analysis

A. Measurement Setup

The setup is shown in Fig. 1. A continuously wavelength tunable laser source is used together with a commercial polarimeter to measure the Jones matrices of the two fibers under test. The laser scans from 1505 to 1565 nm in steps of 0.1 nm, and then the switch toggles and the measurement is repeated on the other fiber under test (FUT). Each FUT is 127 km long and actually a concatenation of two fibers (out of 48) in a 58 km long buried (in 1991), terrestrial cable in Jönköping, Sweden. The fiber is dispersion-shifted with dispersion zero at approximately 1548 nm. The length of the FUT:s were limited by the available power and the sensitivity of the polarimeter. The emitted power was

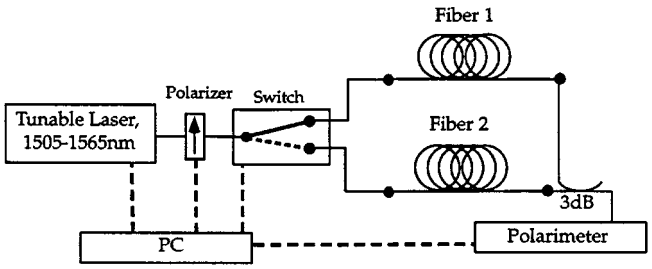

Fig. 1. The measurement set-up.

−3 dBm, and the received power was around −55 dBm. The high degree of polarization of the received signal, 99.5%, was a good indication of that the signal was not too noisy. We also took considerable care to ensure mechanical stability by sticking and taping all loose fiber pieces and patch cords. This, we believe, reduces (if not removes) all rapid fluctuations of the polarization and leave the slower drifts to our investigation. It should be noted, however, that in a real operational system such a mechanical stability can be difficult to maintain, and this will put hard demands on PMD compensators. In our measurement, it was necessary to have short-term (over minutes) stability to ensure that the relatively slow Jones-matrix method would work.

Every 60 nm scan gave 601 Jones matrices and took slightly more than an hour to acquire. The measurement was run for 36 days, which resulted in 388 temporal wavelength traces per fiber. Hence, a total of nearly half a million Jones matrices were acquired during the measurement period. We believe that this is one of the most comprehensive polarization measurements on installed fiber ever performed.

B. Data Analysis

From what will be explained below the data analysis (i.e., to obtain the PMD-vectors from the measured Jones-matrices) was rather cumbersome, involving five steps:

1) identification and removal of erroneous points;
2) identification and removal of sign jumps;
3) sliding average;
4) normalization and removal of PDL;
5) differentiation of Jones matrices and calculation of the PMD-vector.

These steps will be motivated and explained below, but it is instructive to first consider a raw data example. Assume the measured Jones matrix is denoted by

$$J = \begin{bmatrix} A & B \\ C & D \end{bmatrix} \tag{1}$$

where the matrix elements A, B, C, and D are complex numbers. A typical example of traces of some received Jones matrix data can be seen in Fig. 2, which shows the real and imaginary parts of the Jones matrix element A over a 20 nm band, corresponding to 200 measured wavelength points. Ten successive temporal measurements are shown, each separated by approximately 2.2 h. It is evident that the measured data suffers from two kinds of problems, i) erroneous points (around, e.g., 1509–1510 and 1518 nm and ii) sign jumps (at 1508, 1511, 1516, 1516.5, 1519 and 1522 nm). We believe the source of

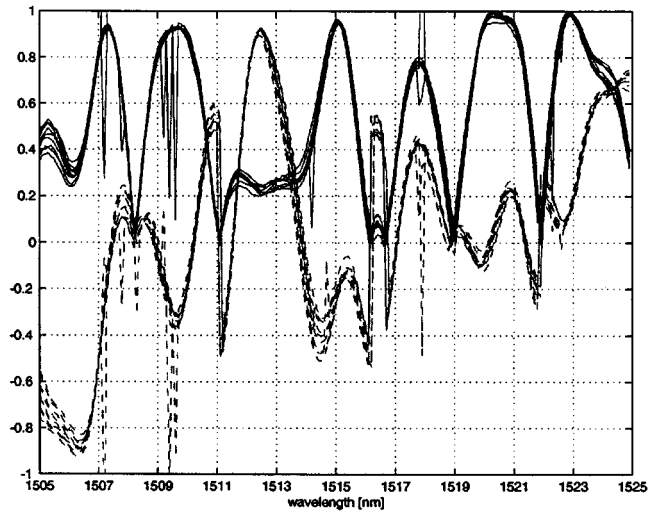

Fig. 2. Example of the measured Jones.matrix raw data. The solid (dashed) line is the real (imaginary) part of the Jones matrix element A. The plot shows ten subsequent measurements (which corresponds to almost a 24-h period) in a 20-nm range, and each 20-nm scan contains 200 points.

those errors to be intrinsic in most Jones matrix measurements, and hence of interest to the "PMD-community," so we will devote some space to a discussion around them.

1) Erroneous Points: The really surprising fact about the erroneous points are that they tend to group in certain wavelength intervals and reappear for also the subsequent measurements (which took place more than two hours later). We have never observed any mode hops in the tunable laser, and are quite certain that that is not the source of error. Instead we trace the erroneous points back to the way the polarimeter determines the Jones matrix. This is done by a method proposed originally by Jones [27], and later used by Heffner [4] in the first paper describing the Jones-matrix measurement method applied to PMD. Before the light is launched into the fiber under test, it is propagated through a polarizer which is oriented at three different positions, 45° apart. The three corresponding Jones vectors after the fiber are measured, and from that data the Jones matrix can be determined, to within a complex constant. Three measurements of the polarization state is therefore necessary, and it is enough that one of these three measurements is wrong to render the complete Jones matrix erroneous. Since the power level is low, the noise background cannot be neglected, and it is plausible that some polarization states are not measured with the same signal-to-noise ratio (SNR) as others. In addition, for certain Jones matrices, small errors in one of the three measured polarization states might give rise to large errors in the computed Jones matrix. Hence some Jones matrices have a greater probability of being wrong than others. Since the temporal change is quite slow (as can be seen in Fig. 2), the erroneous points tend to reappear around certain points in wavelength. In particular, around maxima of the real part of the $(1,\ 1)$-element A (see Fig. 2), the erroneous points seem to be more frequent.

The way to trace and treat the majority of the erroneous points is simple. We use the fact that the fiber has negligible polarization-dependent loss. Then it can be shown that the modulus of all four complex Jones matrix elements must be less than unity.

If some element is above unity that matrix is deemed erroneous, and a new one is obtained by interpolating its nearest (nonerroneous) neighbors.

2) Sign Jumps: The above method to calculate the Jones matrices suffers from the problem that the calculated matrices are not determined with respect to a complex constant [4], [27]. Even though the polarimeter we used normalized the determinant of the matrix to unity, the Jones matrix is still undetermined with respect to sign. The sign is given by the internal algorithm in the polarimeter, which in our case seems to force the real part of the element A to be positive, see Fig. 2. Whenever that element attempts to cross zero, the sign of the entire Jones matrix changes, and obviously most of the other elements will be discontinuous at such a sign jump. In the calculated DGD, this kind of discontinuities will manifest as spurious peaks. Those peaks seem artificial to the user by being discontinuous points on an otherwise continuous plot, but since they are very reproducible, the user might be convinced that they are real data. However, they are indeed artifacts. We believe that this is a generic problem afflicting many commercial instruments using Jones matrix eigenanalysis, of which not many people (manufacturers as well as end users) might be aware. So, rather than leaving the sign of the Jones matrix undetermined, we emphasize that *the sign must be determined by the fact that all Jones matrix elements shall be continuous functions of* λ.

To detect the sign jumps we simply compared the difference and sum between the elements of two consecutive (in wavelength) matrices. At the detected jump points we multiplied all following (in wavelength) matrices with -1.

3) Sliding Average: The above data treatment was almost enough but not completely. A few special cases such as many erroneous points in a row, or erroneous points occurring at or next to a sign jump we deemed "hopeless," and we used a five-point sliding average (in wavelength) to reduce the influence of such points. Note that we put all this effort in reducing discontinuities in the raw Jones matrix data, since they will become very disturbing peaks in the final plots of the PMD-vectors. Two points should be emphasized here: i) The five-point average is not wide enough to destroy the fine structure of the measurements since the PMD correlation length is greater than ten points (1 nm). We will show in the appendix that the correlation length of the PMD vector in our case is approximately 3 nm. ii) It is therefore not very many points that will be significantly affected by this sliding average apart from the really "hopeless" cases, which will be smoothed.

4) PDL Removal: The measured Jones matrices might contain a small amount of PDL due to measurement errors, even after the above data treatment, and this has to be removed before the PMD-vectors could be computed. Mathematically, the Jones matrix must be unitary if the PMD-vector is to be properly defined, but the measured matrices might contain a small amount of PDL that, if not removed will give rise to complex rather than real PMD-vector components.

The mathematical problem is thus: from an arbitrary Jones matrix (in fact any arbitrary 2×2 complex matrix), pick the unitary matrix that is "closest" to the one at hand. We did this in the following way. Every Jones matrix T can be written $T = UH$, where H is a Hermitian matrix accounting for the PDL, and U is a unitary matrix accounting for the polarization rotation (this is known as Jones theorem [28]). We aim to extract U. By multiplying T with its conjugate transpose $T^\dagger$ we get $T^\dagger T = H^\dagger U^\dagger U H = H^2$, since $U^\dagger = U^{-1}$ and $H^\dagger = H$ per definition. By utilizing the properties of Hermitian matrices, we could then uniquely extract H and H^{-1} from H^2, and finally obtain U from $H^{-1}T$. The purist might argue that this way of extracting U from T is not the only way to do it. It is true that other methods might be possible, but the fact is that the PDL-part was in all cases very small; or mathematically: H was in all cases very close to the identity matrix.

5) Differentiation of Jones Matrices: The final step to obtain the PMD-vector is to differentiate the Jones matrices, thus obtaining the PMD-vector from $dT/d\omega T^{-1}$ (see [5] for details). In commercial software for PMD measurement, the numerical differentiation is usually done by the straightforward two-point derivative: $x'_n = (x_{n+1} - x_n)/h$. However, for small step sizes h, this derivative is very sensitive to erroneous points and other sources of noise in the signal. There are two ways to improve the situation. The first is to use a multipoint differentiation formula, and we use here the six-point formula: $x'_n = (x_{n+3} - x_{n-3} - 9(x_{n+2} - x_{n-2}) + 45(x_{n+1} - x_{n-1}))/60h$. The second way of improvement is to use a "fork-derivative," that is, to use, for example, every fifth point of the samples in the differentiation scheme. This decreases the sensitivity to noise by increasing h, but still retains a good resolution in the sense that nearby points have not be computed from the same data. This idea was recently applied to PMD-measurements by Jopson *et al.* [29]. The six-point differentiation formula could then be written $x'_n = (x_{n+15} - x_{n-15} - 9(x_{n+10} - x_{n-10}) + 45(x_{n+5} - x_{n-5}))/300h$, and this was used for our data.

The obvious drawback of this kind of "fork-"differentiation is that the resolution might be reduced, similar to low-pass filtering or sliding average. We took considerable effort to check that this was not the case for our data. We compared the plot of DGD as a function of wavelength for increasing number of samples separating the points in the differentiation formula, just to make sure that we did not filter away the fine structure of the wavelength variation in the PMD. We found that in our case, the six-point differentiation scheme on every fifth point did a good job of removing spurious peaks due to measurement errors without reducing the resolution.

III. Measurement Results

After the above data treatment, we are ready to analyze the data. Contour plots of the measured DGD versus wavelength and time are shown in Fig. 3. There is nothing unusual in those plots besides the fact that some very sudden changes occur (for both fibers) around days 8, 18, 20, 30, and 36. We discuss those features in some more detail below.

Some straightforward averages were also done right away on the data. The DGD averaged over wavelength and time was found to be 2.75 and 2.89 ps for the two fibers, which corresponds to PMD-coefficients of 0.24 and 0.26 ps/$\sqrt{\text{km}}$. The average over wavelength varied $\pm 10\%$ around those values. The average over time showed a more significant fluctuation as can

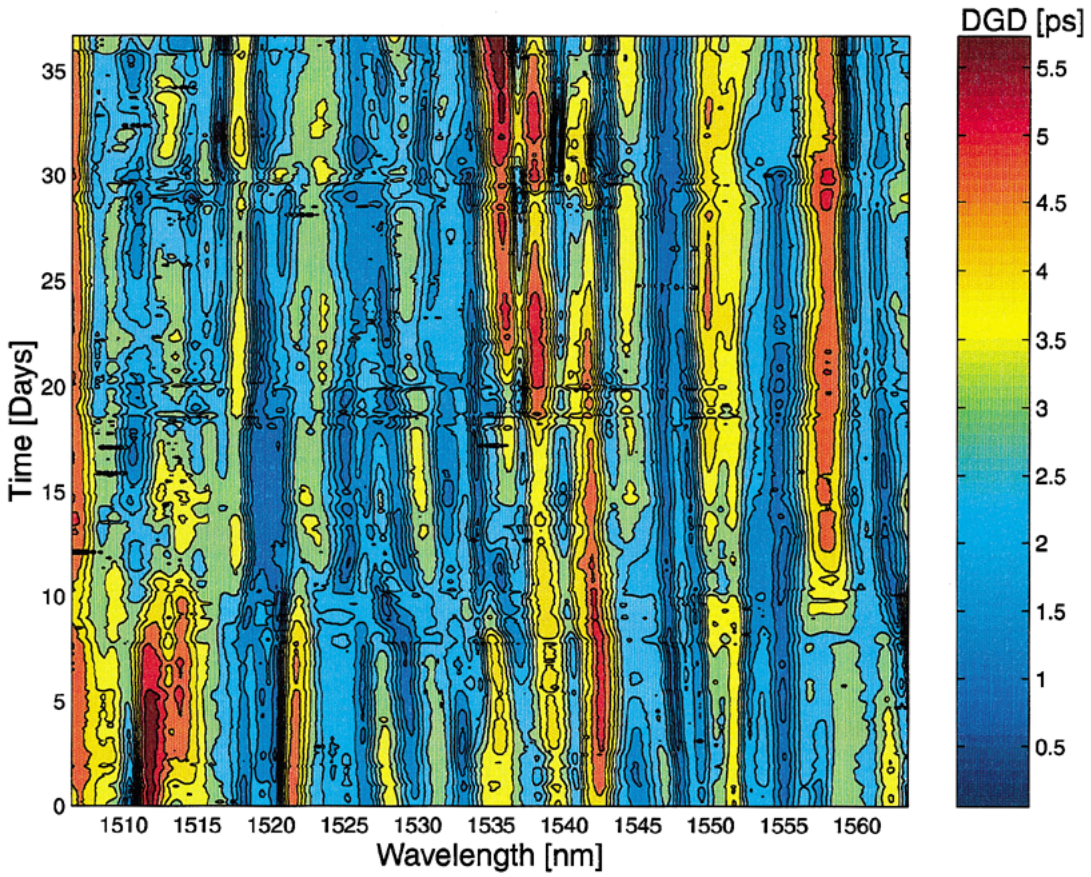

Fig. 3. DGD versus time and wavelength of fiber 1.

be seen in Fig. 4. This indicates that over the 36 days measurement period, the temporal drift was not significant enough to realize any reliable statistical averages. In the wavelength direction, however, this was the case.

Another interesting point, that has so far received very little attention in the literature, is the isotropicity of the PMD-vector. That is, is any direction in Stokes space preferred, or is the PMD-vector isotropically distributed, as most theoretical approaches assume? This is by no means obvious, since telecom fibers are believed not to have any intrinsic circular birefringence [3]. The isotropicity has only been verified on few occasions, and then with very limited data [30]. According to the statistical theory for PMD [1], each of the three components of the PMD-vector is a superposition of many small random variables, which, according to the central limit theorem, would give them a Gaussian distribution. Moreover, if the PMD-vector is isotropic, then the three components would have identical Gaussian probability distribution functions. In Fig. 5, we verify this, and it is evident that histograms over the three components of the measured PMD-vectors are very close to the theoretically predicted Gaussian (dashed line in the figures). The agreement is fairly good, although not excellent. Particularly in the wings of the distributions significant deviations from the Gaussians can be found. This implies that the DGD has a Maxwellian distribution, apart from in the wings. Deviations from the Maxwellian distribution in the wings have also been seen in other measurements [21]. Partly this can be expected from the limited amount of samples far out in the wings, and partly by measurement errors. However, it might also be that a more refined theory is needed to explain the deviations in the wings of the Gaussians, but for the moment we lack other explanations of these deviations from the theory.

The basic aim with the setup was to compare the temporal drifts between the two fibers. We found it most relevant to compute the changes in the PMD-vector from one time point to the next, and then average this change over the entire wavelength range. For the length of the PMD vector (the DGD) we thus computed

$$E\left[\left|\frac{|\boldsymbol{\Omega}(t+\Delta t,\,\lambda)|-|\boldsymbol{\Omega}(t,\,\lambda)|}{\Delta t}\right|\right]_{\lambda} \tag{2}$$

where $E[\ ]_{\lambda}$ denotes averaging over wavelength, and Δt is the time between two successive measurement instants, which was approximately 2.2 hours. For the angular changes, i.e., the PSP drift, we computed the average angle between two successive PMD vectors, i.e.

$$E\left[\arccos\left(\frac{\boldsymbol{\Omega}(t+\Delta t,\,\lambda)\cdot\boldsymbol{\Omega}(t,\,\lambda)}{|\boldsymbol{\Omega}(t+\Delta t,\,\lambda)|\,|\boldsymbol{\Omega}(t,\,\lambda)|}\right)\frac{1}{\Delta t}\right]_{\lambda}. \tag{3}$$

The averaged change in DGD and in PSP-angles are shown in Fig. 6. It is clear from these plots that there is a remarkable agreement between the two fibers with respect to the average change of both the PSP's and the DGD. In fact, we calculated a correlation coefficient between the two fibers of 96%, both

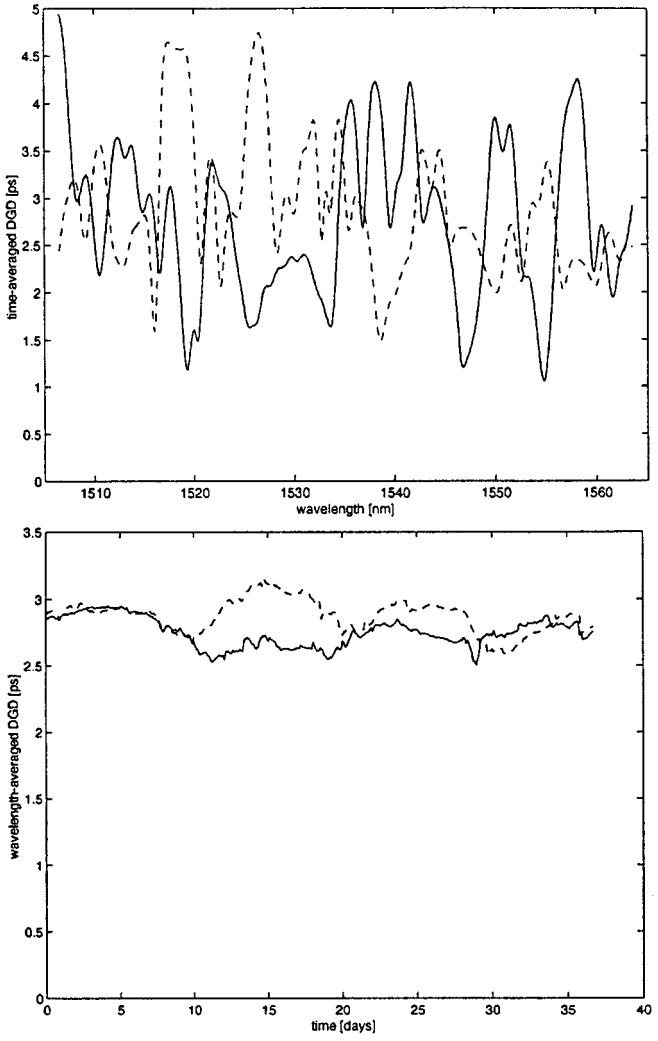

Fig. 4. Top: The DGD averaged over time and plotted as a function of wavelength. Bottom: The DGD averaged over wavelength and plotted as a function of time. The solid line is fiber 1 and the dashed line is fiber 2.

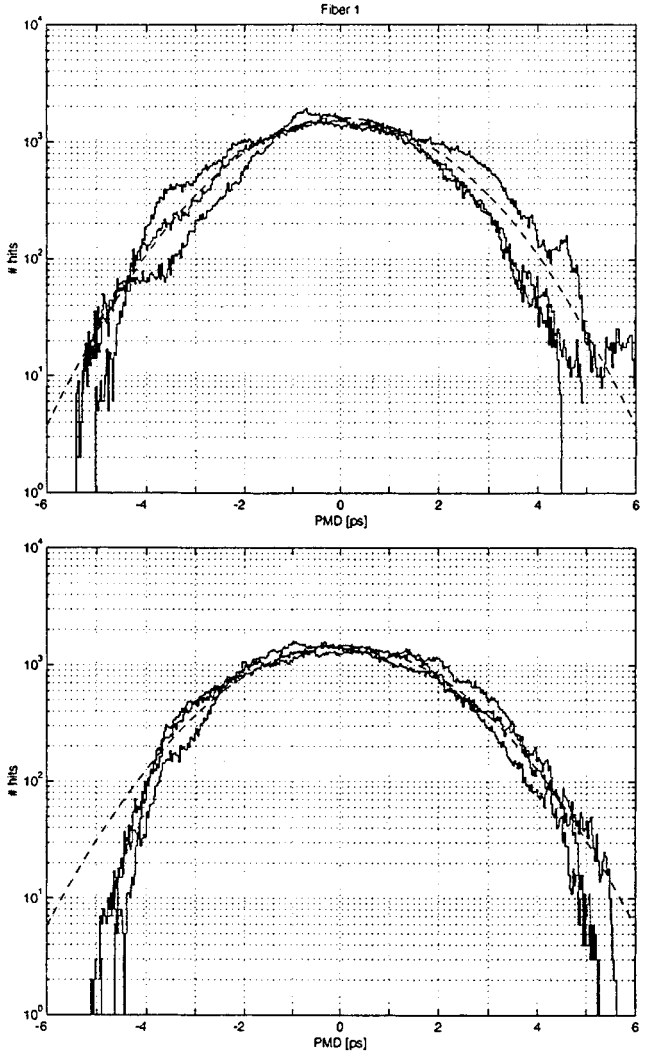

Fig. 5. Histograms over the three PMD-vector components (solid) for each fiber. The dashed lines are Gaussian fits.

for the change in DGD and the change in PSP. Even though the fibers are located in the same cable, they are distinct, and it is a bit surprising to find the PMD drift in the two fibers to be so well correlated. From Fig. 6, we can also quantify the average drift to be around 10% per day for the DGD, and to be around 20° per day for the angular change of the PSP:s. Also, we note that there is a strong correlation between the changes in DGD and PSP. A large change in the DGD is accompanied with a large change in the PSP's, and this is just in agreement with the discussion on polarization drift from Section I-B above, where it was argued that perturbations around the middle of the FUT affects the DGD most, and perturbations near the endpoints mostly affects the PSP's. If the perturbations are evenly distributed along the fiber, then we will see changes in the DGD and PSP:s simultaneously. The physical reason for the drifts we attribute to changes in the temperature during the measurement period. Since we observed very few rapid changes of the PMD, we believe mechanical perturbations to have been more or less eliminated by carefully sticking all loose fibers. The temperature data in Fig. 6 indicates that there is a certain amount of correlation between the temperature changes and the PMD-change. This might seem surprising since the air temperature should not affect a buried cable. However, at 6 hub stations along the 58 km cable, the cable enters the air for some tens of meters. We believe that this exposure to air temperature is enough to cause the drift, and this fact have also been verified in previous measurements by De Angelis *et al.* [18]. Therefore, a submarine cable in the stable environment at the bottom of the ocean would not give rise to very much drift, but the parts of the cable leaving or entering the deep ocean are exposed to water currents and temperature changes and might therefore contribute to the PMD-drift. On the other hand, aerial fiber cables are heavily exposed to mechanical perturbations from wind, in addition to the temperature changes, and the PMD of such cables can be expected to vary on a very short time scale.

IV. Statistical Properties of the Drift

When discussing the properties of the temporal drift it is two things that must be distinguished. They are first, the drift of the absolute polarization state, and secondly the drift of the PMD-

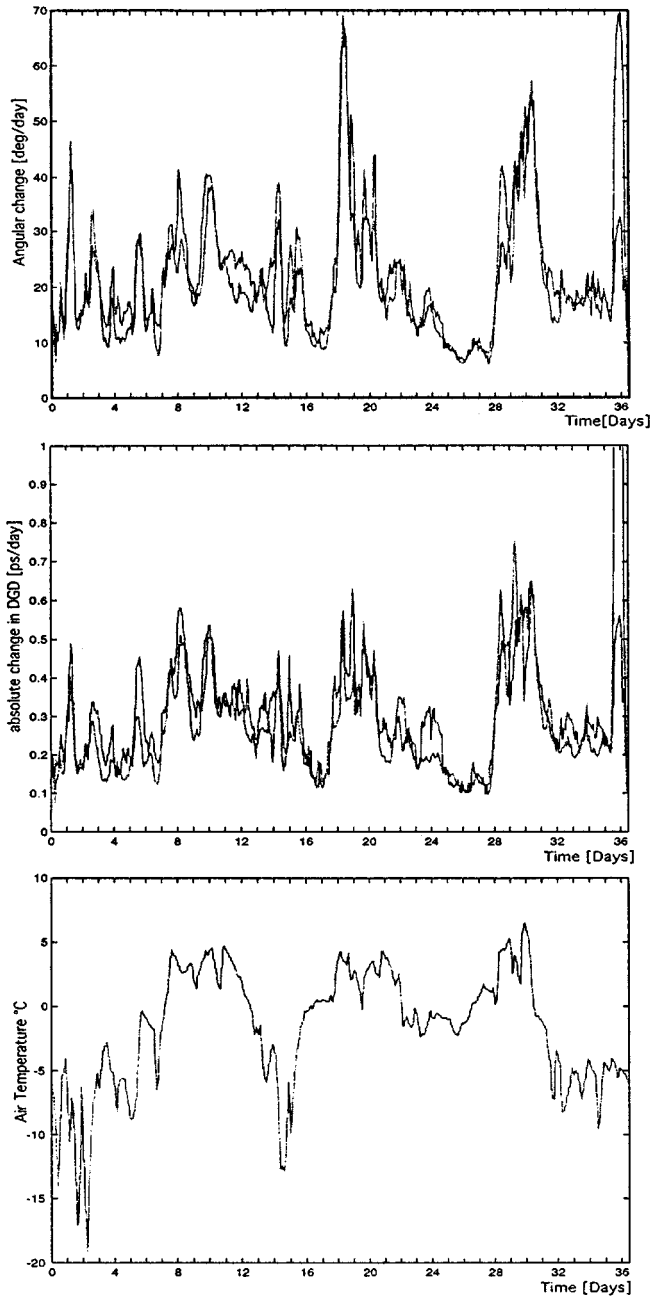

Fig. 6. The average (over wavelength) change in the PMD-vector angle (upper) and PSP (middle) with time for fiber 1 (solid) and fiber 2 (dotted). The bottom figure plots the air temperature in the Jönköping area over the measurement period.

vector. We will consider these drifts separately, and also show how they are related.

From a mathematical point of view, it is convenient to treat the drift in terms of correlation functions, i.e. to answer the question "How well are two polarization states at time instances t_1 and t_2 correlated?". We define the auto correlation function (ACF) for the absolute polarization states (or more specifically for the Mueller matrices) as $G_M = E[M^t(\omega_1, t_1)M(\omega_2, t_2)]$, where superscript t denotes transpose. A measure of the correlation between two polarization states at those time instances and frequencies would then be their statistically expected scalar product, i.e., $E[\boldsymbol{s}(\omega_1, t_1) \cdot \boldsymbol{s}(\omega_2, t_2)] = \boldsymbol{s}_0^t G_M \boldsymbol{s}_0$ where $\boldsymbol{s}_0$ is the input polarization state into the fiber. The derivation of G_M is lengthy and deferred to the appendix. We quote here two important special cases, namely when the polarization states are at the same time ($t_1 = t_2$) or at the same frequency ($\omega_1 = \omega_2$). Hence, the decorrelation in time will be

$$E[\boldsymbol{s}(t_1) \cdot \boldsymbol{s}(t_2)] = \exp\left(-\frac{|\Delta t|}{t_d}\right) \tag{4}$$

where $\Delta t = t_1 - t_2$, and t_d is the typical drift time for the absolute polarization states. This is a coefficient that is unique for each fiber, and has to be measured. How it scales with PMD and fiber length, together with the assumptions leading up to this formula is discussed in the Appendix. The decorrelation in wavelength will be

$$E[\boldsymbol{s}(\omega_1) \cdot \boldsymbol{s}(\omega_2)] = \exp\left(-E[\Delta\tau^2]\frac{\Delta\omega^2}{3}\right) \tag{5}$$

where $\Delta\omega = \omega_1 - \omega_2$. This result is remarkably useful as it directly demonstrates how the decorrelation in frequency (or wavelength) is related to the average DGD of the fiber. We will defer a thorough discussion of this relation to future work, since here we are more interested in the effects of the temporal drift, i.e., (4). The assumptions leading to that formula are i) that we are in the strong mode-coupling regime where the DGD grows with the square root of the fiber length and ii) temperature variations in the index difference between the fast and slow polarization states is the main cause of the drift.

The next step is to derive the ACF for the PMD-vector. This can also be done in time and wavelength, but the wavelength ACF was recently derived in Ref [6], so we focus here on the temporal drift properties. Again the details can be found in the appendix, and the main result is

$$E[\boldsymbol{\Omega}(t_1) \cdot \boldsymbol{\Omega}(t_2)] = E[\Delta\tau^2]\frac{1 - \exp\left(-\frac{|\Delta t|}{t_d}\right)}{|\Delta t|/t_d}. \tag{6}$$

By comparing the functional forms of the two derived auto correlation functions [(4) and (6); we see that the Mueller ACF is slightly more peaked and has an exponential decay, whereas the PMD ACF has a slower, algebraic decay. This is evident from Fig. 7, in which the two functions are compared. They are, however, both determined by the timescale t_d so this result is in good agreement with the discussion in Section I-B.

The coefficient t_d gives a measure of the average drift time of both the absolute polarization states and the PMD-vector of a installed fiber. This parameter cannot be expected to be predicted or estimated from known fiber parameters, since it depends on installation-specific data such as the amount of environmental perturbations and disturbances. In the appendix we show that t_d depends on the PMD via $t_d = 2t_0/(3\omega^2 E[\Delta\tau^2])$, where ω is the carrier frequency, and t_0 is a measure of the drift time of the index difference in the birefringent element used to model the fiber. This relation clearly shows that the typical drift time t_d decreases with the PMD. The parameter t_0 is an individual parameter characterizing any installed fiber, but it is more practical to directly measure t_d than t_0 for all systems of interest. The relevance of our theoretical analysis lies in i) that it shows explic-

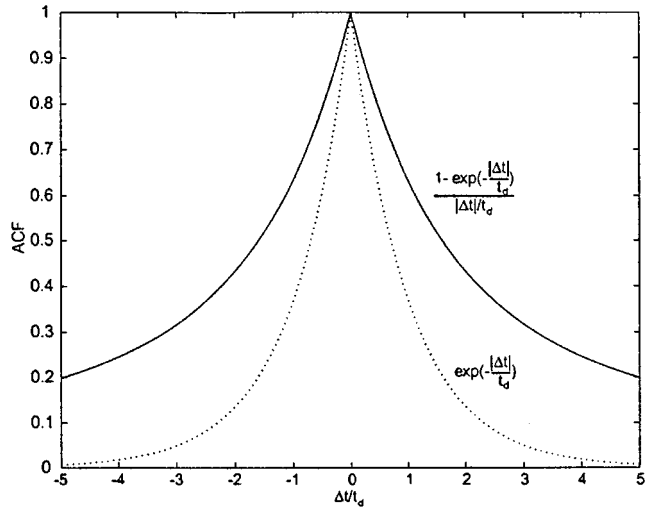

Fig. 7. A comparison between the derived temporal ACF's for the absolute polarization state [(4), dotted], and the PMD vector [(6), solid], show that the former has a much more rapid exponential decay.

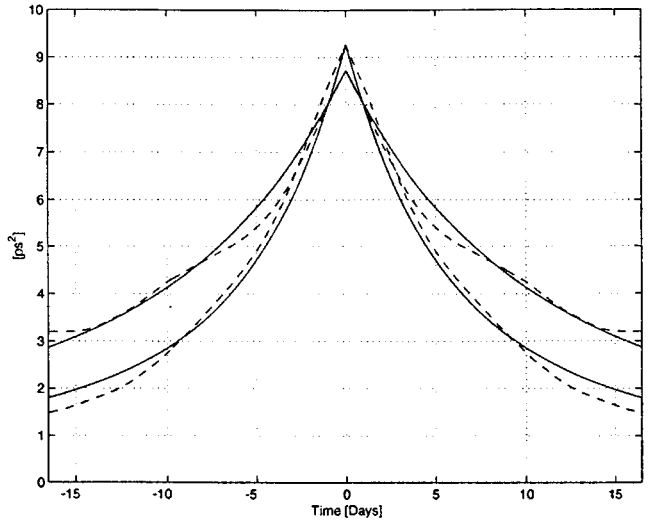

Fig. 8. The measured autocorrelation function of the DGD for the two fibers (solid) and the theoretical autocorrelation function from (6) (dashed). We have used the characteristic drift times equal to respectively $t_d = 3.0$ and 5.7 days

itly how the temporal drift t_d scales with the amount of PMD and ii) that it shows how the drift time of the absolute polarization state is connected to the drift time of the PMD-vector. The absolute drift is much easier to measure than the PMD-vector drift, so this might be of practical interest. Moreover, the outage time [21] in a PMD-limited system can be expected to be of the order of this drift time. In Fig. 8 we have plotted the measured and theoretical ACF's for the PMD-vectors, using $t_d = 3.0$ and 5.7 days for the respective fibers. The agreement is quite good, but the reader should note that we have had a free fitting parameter in t_d. The explanation for the difference in drift times for the two fibers is that not all of the fibers in the cable enter all hub stations, so different fibers are exposed to different amounts of temperature changes. This is another indication of that the time scale is an important, individual characteristic parameter that should be measured together with the PMD for all fibers.

V. Conclusion

In conclusion, we have described the result of what we believe to be the most detailed long-term measurement of PMD ever reported. We have discussed the treatment of the measured data and identified some crucial points that should be of interest to manufacturers as well as end users. Then we focused the discussion on the temporal drift, and derived a theory to account for both the drift of the absolute polarization state, and that of the PMD-vector. Perhaps more importantly, we showed how the drift time is related to the well-known fiber properties, like the PMD-coefficient. The theory was found to agree reasonably well with measurements.

Appendix
Derivation of the Autocorrelation Functions

In order to further quantify the drift we will first compute the auto correlation function of the Mueller matrix of the fiber (which will give information about the drift of the absolute polarization state). In a second stage we will compute the drift and autocorrelation properties of the PMD-vector. Recently, this was done with respect to wavelength [6], but now we will generalize that approach to account also for the temporal drift.

A. The ACF for the Mueller Matrices

We will base the derivation of the ACF on the discrete model of the fiber, in which the fiber is modeled as a concatenation of birefringent pieces each having a constant birefringence. Then we will perform the statistical average (by averaging over all possible birefringence axes), and finally go to a continuous-fiber limit by allowing each fiber piece to shrink to an infinitesimal length. This final step is not necessary, but it provides some very elegant and compact formulas which, as we shall see, agree quite well with experiments. This approach have also the benefit of resolving a problem (the Stratonovich–Ito ambiguity) connected with the integration of stochastic infinitesimals [1]. The drawback of this approach is that it is restricted to the strong mode-coupling limit only, where the DGD grows as the square root of the fiber length.

Hence, in terms of Mueller matrices, the fiber consists of N birefringent pieces of length L_0. The average squared DGD of such a concatenation can be written as $E[\Delta\tau^2] = NL_0^2\Delta n^2/c^2$, where Δn is the index difference between the slow and fast axes of each birefringent fiber piece, and c the speed of light in vacuum. Each element in the concatenation has a birefringence axis $\boldsymbol{e}_k$ in Stokes space, so that its Mueller matrix M_k can be written conveniently using the matrix exponential as $M_k = \exp[\gamma_k(\omega)\boldsymbol{e}_k\times]$. Here the notation $\boldsymbol{e}_k\times = (x_k, y_k, z_k)\times$ should be interpreted as the skew-symmetric matrix corresponding to the cross-product operator (see e.g. Refs. [6], [7]), and the matrix exponential is defined by its Taylor expansion. The retardation $\gamma_k(\omega)$ equals $\omega\Delta n_k L_0/c$, where we allow for the possibility of having different Δn in each piece. The Mueller matrix of the entire fiber we denote by M^N, and it is $M^N = M_N M_{N-1}\cdots M_2 M_1$.

At this point, we should stop to discuss the physical model. We will make a few simplifying assumptions. Firstly, we assume

that the index difference Δn and the birefringence axis $\boldsymbol{e}_n$ are independent of the optical frequency. This is no crucial restriction, since any fiber can be realized by including sufficiently many small birefringent pieces. The second assumption is that the time dependence enters via a random drift in the index difference only. In principle, the birefringence axes might also drift, but this is more complex to treat analytically, so we limit this work to a drift in Δn only. This is also physically consistent with the fact that for birefringent waveplates and polarization maintaining fibers, a temperature change (which we identify as the main source of the drift) will cause a change in the index difference rather than the polarization eigenaxes.

We are now ready to calculate the autocorrelation function $G_{M,N}$ of the first N Mueller matrices

$$G_N = E[M^N(t_1, \omega_1)(M^N(t_2, \omega_2))^{-1}] = \prod_{k=1}^{N} I \frac{1 + 2E[\cos(\Delta_k)]}{3} \tag{7}$$

where $\Delta_k = (\omega_1 \Delta n_k(t_1) - \omega_2 \Delta n_k(t_2))L_0/c$, I is the unity matrix, and the expectation value $E[\ ]$ means averaging over birefringence axes and index differences. The last equality arose from averaging the birefringence axis b_k uniformly over all possible directions. This was done by utilizing the formula $\exp(ab\times) = I + \sin(a)b\times + (1 - \cos(a))b\times b\times$ (see e.g. [31]) together with $E[b\times] = 0$ and $E[b \times b\times] = -2I/3$. The next step is to average the $\cos(\Delta_k)$-term, which is simplified if we assume the number of independent fiber pieces N to be very large. This implies that $L_0 = L/N$ is so small that $\cos(\Delta_k) \approx 1 - \Delta_k^2/2$. Taking the expectation value of this yields $E[\Delta_k^2] = (E[\Delta\tau^2]/N)(\omega_1^2 + \omega_2^2 - 2\omega_1\omega_2 f(t_1 - t_2))$, where $f(t_1 - t_2) = f(\Delta t) = E[\Delta n(t_1)\Delta n(t_2)]/E[\Delta n^2]$ is the autocorrelation function of the temporal drift of the index difference. Hence, we end up with

$$G_{M,N} = I\left(1 - E[\Delta\tau^2]\frac{\omega_1^2 + \omega_2^2 - 2\omega_1\omega_2 f(\Delta t)}{3N}\right)^N \tag{8}$$

and in the limit $N \to \infty$ we are left with $G_M = Ig_M(\omega_1, \omega_2, \Delta t)$ where g_M is the Mueller matrix ACF, given by

$$g_M(\omega_1, \omega_2, \Delta t) = \exp\left(-E[\Delta\tau^2]\frac{\omega_1^2 + \omega_2^2 - 2\omega_1\omega_2 f(\Delta t)}{3}\right). \tag{9}$$

From this expression we can extract some important information about the polarization drift properties of the fiber. Putting, e.g., $\omega_1 = \omega_2 = \omega$ gives $g = \exp(-E[\Delta\tau^2]\omega^2(1 - f(\Delta t))2/3)$. In this expression, the dimensionless factor $\alpha = E[\Delta\tau^2]\omega^2$ is usually very large, since the DGD is in the picosecond range and the optical period $2\pi/\omega$ is 5.2 fs at a wavelength of 1.55 μm. Hence, α is around $10^3 - 10^8$ for most cases of interest. This reflects the fact that only a very small change in the index difference will give rise to a large change in the absolute polarization state. Then, obviously only the parts of the function f that are close to unity is of interest, and if we write it using its Taylor expansion $f(\Delta t) \approx 1 - |\Delta t|/t_0$, the ACF for the Mueller matrixes reduces to

$$g_M = \exp\left(-\frac{|\Delta t|}{t_d}\right) \tag{10}$$

where the typical drift time $t_d = t_0/\alpha$ is an individual parameter that has to be measured for each link under study. However, we can draw one general conclusion from $t_d = 2t_0/(3\omega^2 E[\Delta\tau^2]) = 2t_0/(3\omega^2 \mathrm{PMD}^2 z)$, where PMD is the PMD-coefficient (in ps/$\sqrt{\text{km}}$) of the fiber. This is that the drift is more rapid for long fibers and high PMD, something which has been conjectured but not proven until now. We note again the main assumptions leading to this conclusion; 1) that the index difference is the main cause of the drift and 2) we are in the strong mode-coupling regime. A similar result was obtained in a theoretical study by Imai and Matsumoto [11]. They considered the variance of the random motion of the polarization state on the Poincaré sphere, using a similar model as the one here (i.e., modeling the fiber as a concatenation of shorter pieces). Their model is slightly more limited since several simplifying assumption limiting the motion to be small on the sphere were necessary. Our model is more general in that it computes the ACF explicitly, accounts for frequency deviations between the Mueller matrices, and directly connects the drift with the average PMD of the fiber. The important conclusions regarding how the drift scales with fiber length is however the same between the two models.

B. The ACF for the PMD-Vector

We will now apply a similar method as the one above to derive the ACF for the PMD vector. Mathematically speaking, what we aim to compute is

$$g_\Omega(t_1, t_2, \omega_1, \omega_2) = E[\boldsymbol{\Omega}(t_1, \omega_1) \cdot \boldsymbol{\Omega}(t_2, \omega_2)] \tag{11}$$

that is the expectation of the scalar product of two PMD-vectors at different frequencies and/or times. We assume the same concatenated fiber model as above. The PMD-vector $\boldsymbol{\Omega}^k$ of the first k fiber pieces can now be written in terms of the Mueller matrices as [1]: $\boldsymbol{\Omega}^k\times = dM^k/d\omega(M^k)^{-1}$, and it is possible to derive the Gisin–Pellaux recursion relation [5] for the kth PMD-vector according to:

$$\boldsymbol{\Omega}^k = \frac{d\gamma_k}{d\omega}\boldsymbol{e}_k + M_k\boldsymbol{\Omega}^{k-1}. \tag{12}$$

This formula is a very elegant result for concatenation of PMD-vectors and it can be generalized and stated as: *The PMD vector of a concatenation of birefringent elements is the vector sum of all ingoing PMD-vectors, transformed by the adequate Mueller matrices to the same position*. It is quite remarkable that the reduction of the rather complicated formula given by Gisin and Pellaux to the above simple and physically appealing form was unnoticed until [6]. However, a particular integral form of the concatenation rule, although less general than above, was given by Mollenauer and Gordon in 1994 [32].

We will now calculate the ACF of the PMD-vector after N fiber pieces, i.e., $E[\boldsymbol{\Omega}^N(\omega_1, t_1) \cdot \boldsymbol{\Omega}^N(\omega_2, t_2)] = g_{\Omega,N}(\omega_1, \omega_2, t_1, t_2)$. By using the recursion formula, (12) and

carrying out the averaging process over $\boldsymbol{e}_n$, we get a recursion relation for the autocorrelation

$$g_{\Omega,N} = E\left[\frac{d\gamma_N}{d\omega}(\omega_1, t_1)\frac{d\gamma_N}{d\omega}(\omega_2, t_2) + a(\Delta_N)g_{N-1}(\omega_1, \omega_2)\right] \quad (13)$$

where $a(\Delta_N) = (1 + 2\cos(\Delta_N))/3$ and Δ_N is defined as above. The remaining average expressed in this equation is over Δn, and we note that when the number of birefringent fiber pieces is large enough we can Taylor expand the function a so that

$$E[a(\Delta_N)] \approx 1 + E\left[\frac{\Delta_N^2}{3}\right]. \quad (14)$$

This average was performed previously in connection with (8). We are finally in position to solve the recursion equation (13). The solution is

$$g_{\Omega,N} = E\left[\frac{d\gamma_N}{d\omega}(\omega_1, t_1)\frac{d\gamma_N}{d\omega}(\omega_2, t_2)\right]\frac{1 - E[a]^N}{1 - E[a]}. \quad (15)$$

Finally, we take the limit $N \to \infty$ so that the final PMD-vector ACF $g_\Omega(\omega_1, \omega_2, \Delta t)$ can be expressed in terms of the Mueller-matrix ACF g_M from (9) as

$$g_\Omega = E[\Delta\tau^2]f(\Delta t)\frac{g_M - 1}{\ln(g_M)} \quad (16)$$

where $f[\Delta t]$ is the index-difference ACF that was defined in connection with (9).

The special case $\Delta t = 0$ was investigated in [6], where it was found that the frequency ACF had a width of the order of the inverse average DGD. In the measurements reported in the previous section $E[\Delta\tau]$ was approximately 2.8 ps, which corresponds to a bandwidth of 2.7 nm. Hence, the PMD vector varies randomly with a correlation length of almost 3 nm, which verifies that a signal manipulation such as the sliding average over a 0.5-nm band discussed in Section II will not significantly affect the measured data.

We focus now instead on the pure temporal drift, i.e., the special case $\omega_1 = \omega_2 = \omega$. Just as in the discussion on the properties of g_M above, the coefficient $\alpha = E[\Delta\tau^2]\omega^2$ is very large, and the ACF can then be approximated with

$$g_\Omega = E[\Delta\tau^2]\frac{1 - \exp\left(-\dfrac{|\Delta t|}{t_d}\right)}{|\Delta t|/t_d}. \quad (17)$$

We should at this point stress a few known statistical properties of the stochastic vector process $\boldsymbol{\Omega}(\omega)$ [1], [2], and what new information we have gained. First, $\boldsymbol{\Omega}$ consists of three *independent* stochastic processes: $\Omega(\omega) = (\Omega_x(\omega), \Omega_y(\omega), \Omega_z(\omega))$ so that cross correlations among those are zero, e.g., $g_{xy}(\omega_1, \omega_2) = E[\Omega_x(\omega_1)\Omega_y(\omega_2)] = 0$. Second, due to the fact that all birefringence vectors are uniformly directed in space, the statistical properties of $\boldsymbol{\Omega}$ will be spherically symmetric. Therefore $g_{xx} = g_{yy} = g_{zz} = g_\Omega/3$. This isotropicity would not hold if the fiber were modeled differently, e.g., if the birefringence axes $\boldsymbol{e}_n$ were randomly distributed in the $x - y$ plane only. In fact it has been shown that the absolute polarization state will approach the uniform spread in that kind of model [3]. It is therefore plausible that at sufficiently long distances, the PMD vector of also such a model would be uniformly distributed over the Poincaré sphere.

ACKNOWLEDGMENT

The authors would like to acknowledge H. Vedin at the Swedish Institute for Hydrology and Meteorology (SMHI) for supplying the temperature data.

REFERENCES

[1] G. J. Foschini and C. D. Poole, "Statistical theory of polarization mode dispersion in single mode fibers," *J. Lightwave Technol.*, vol. 9, pp. 1439–1456, 1991.
[2] N. Gisin, "Solution of the dynamical equation for polarization dispersion," *Opt. Commun.*, vol. 86, pp. 371–373, 1991.
[3] P. K. A. Wai and C. R. Menyuk, "Polarization mode dispersion, decorrelation and diffusion in optical fibers with randomly varying birefringence," *J. Lightwave Technol.*, vol. 14, p. 148, 1996.
[4] B. L. Heffner, "Automated measurement of polarization mode dispersion using jones matrix migenanalysis," *IEEE Photon. Technol. Lett.*, vol. 4, pp. 1066–1069, 1992.
[5] N. Gisin and J. P. Pellaux, "Polarization mode dispersion: Time versus frequency domains," *Opt. Commun.*, vol. 89, pp. 316–323, 1992.
[6] M. Karlsson and J. Brentel, "The autocorrelation function of the pmd-vector," *Opt. Lett.*, vol. 24, pp. 939–941, 1999.
[7] M. Karlsson, "Polarization mode dispersion induced pulse broadening in optical fibers," *Opt. Lett.*, vol. 23, pp. 688–690, 1998.
[8] R. A. Harmon, "Polarization stability in long lengths of monomode fiber," *Electron. Lett.*, vol. 18, pp. 1058–1060, 1982.
[9] K. Mochizuki, Y. Namihira, H. Yamamoto, and Y. Ejiri, "Polarization mode dispersion and polarization stability in an optical fiber submarine cable," in *Proc. Optic. Fiber Commun. Conf. (OFC'83)*, 1983, Paper 29A4-3.
[10] K. Myogadani, S. Tanaka, and Y. Suetsugu, "Polarization fluctuation in single mode fiber cables," in *Proc. 11th European Conf. Optic. Commun. (ECOC'85)*, 1985, pp. 151–154.
[11] T. Imai and T. Matsumoto, "Polarization fluctuations in single-mode optical fiber," *J. Lightwave Technol.*, vol. 6, pp. 1366–1375, 1988.
[12] G. Nicholson and D. J. Temple, "Polarization fluctuation measurements on installed single-mode optical fiber cables," *J. Lightwave Technol.*, vol. 7, pp. 1197–1200, 1989.
[13] C. D. Poole, N. S. Bergano, H. J. Schulte, R. E. Wagner, V. P. Nathu, J. M. Amon, and R. L. Rosenberg, "Polarization fluctuations in a 147 km undersea lightwave cable during installation," *Electron. Lett.*, vol. 23, pp. 1113–1115, 1987.
[14] Y. Namihira and H. Wakabayashi, "Real-time measurements of polarization fluctuations in an optical fiber submarine cable in a deep-sea trial using electooptic $linio_3$ device," *J. Lightwave Technol.*, vol. 7, pp. 1201–1206, 1989.
[15] T. Imai, Y. Terasawa, and Y. Ohtsuka, "Polarization fluctuations characteristics of a highly birefringent fiber system under forced vibration," *J. Lightwave Technol.*, vol. 6, pp. 720–727, 1988.
[16] Y. Namihira, Y. HHoriuchi, S. Ryu, K. Mochizuki, and H. Wakabayashi, "Dynamic polarization fluctuation characteristics of optical fiber submarine cables under various environmental conditions," *J. Lightwave Technol.*, vol. 6, pp. 728–738, 1988.
[17] C. D. Poole, R. W. Tkach, A. R. Chraplyvy, and D. A. Fishman, "Fading in lightwave systems due to polarization-mode dispersion," *IEEE Photon. Technol. Lett.*, vol. 3, pp. 68–70, 1991.
[18] C. De Angelis, A. Galtarossa, G. Gianello, F. Matera, and M. Schiano, "Time evolution of polarization mode dispersion in long terrestrial links," *J. Lightwave Technol.*, vol. 10, pp. 552–555, 1992.
[19] T. Takahashi, T. Imai, and M. Aiki, "Time evolution of polarization mode dispersion in 120 km installed submarine cable," *Electron. Lett.*, vol. 29, pp. 1605–1606, 1993.
[20] M. Murakami, T. Takahashi, M. Aoyama, T. Imai, M. Amemiya, M. Sumida, and M. Aiki, "System performanc evaluation of the fsa submarine optical amplifier system," *J. Lightwave Technol.*, vol. 14, pp. 2657–2671, 1996.

[21] H. Bülow and G. Veith, "Temporal dynamics of error-rate degradation induced by polarization-mode dispersion fluctuation of a field fiber link," in *Proc. European Conf. Optic. Commun. (ECOC'97)*, 1997, pp. 115–118.
[22] J. Cameron, L. Chen, X. Bao, and J. Stears, "Time evolution of polarization mode dispersion in optical fibers," *IEEE Photon. Technol. Lett.*, vol. 10, pp. 1265–1267, 1998.
[23] H. Bülow, W. Baumert, H. Schmuck, F. Mohr, T. Schulz, F. Küppers, and W. Weiershausen, "Measurement of the maximum speed of pmd fluctuation in installed field fiber," in *Proc. Optic. Fiber Commun. Conf. (OFC'99)*, 1999.
[24] C. D. Poole, N. S. Bergano, R. E. Wagner, and H. J. Schulte, "Polarization dispersion and principal states in a 147 km undersea lightwave cable," *J. Lightwave Technol.*, vol. 6, pp. 1185–1189, 1988.
[25] L. M. Gleeson, E. S. R. Sikora, and M. J. O'Mahoney, "Experimental and numerical investigation into the penalties induced by second-order polarization mode dispersion at 10 gb/s," in *Proc. European Conf. Optic. Commun. (ECOC'97)*, 1997, pp. 15–18.
[26] T. Kawasawa and Y. Namihira, "Long-term polarization mode dispersion measurement of installed optical submarine cable," in *Proc. Optic. Fiber Commun. Conf. (OFC'94)*, 1994, pp. 228–229.
[27] R. C. Jones, "A new calculus for the treatment of optical systems vi. experimental determination of the matrix," *J. Opt. Soc. Amer.*, vol. 37, pp. 110–112, 1947.
[28] H. Hurwitz Jr. and R. C. Jones, "A new calculus for the treatment of optical systems II. Proof of three general equivalence theorems," *J. Opt. Soc. Amer.*, vol. 31, pp. 493–499, 1941.
[29] R. M. Jopson, L. E. Nelson, and H. Kogelnik, "Measurement of second-order polarization-mode dispersion vectors in optical fibers," *IEEE Photon. Technol. Lett.*, vol. 11, pp. 1153–1155, 1999.
[30] C. D. Poole, J. H. Winters, and J. A. Nagel, "Dynamical equation for polarization mode dispersion," *Opt. Lett.*, vol. 16, pp. 372–374, 1991.
[31] K. N. S. Rao, *Linear Algebra and Group Theory for Physicists*. New York: Wiley, 1996.
[32] L. F. Mollenauer and J. P. Gordon, "Birefringence-mediated timing jitter in soliton transmission," *Opt. Lett.*, vol. 19, pp. 375–377, 1994.

Magnus Karlsson, photograph and biography not available at the time of publication.

Jonas Brentel, photograph and biography not available at the time of publication.

Peter. A. Andrekson (S'84–M'88), photograph and biography not available at the time of publication.